Control and Cybernetics

vol. **43** (2015) No. 3

Transfer function–based impulse response analysis for a class of hyperbolic systems of balance laws*

by

Krzysztof Bartecki

Institute of Control and Computer Engineering
Opole University of Technology
ul. Sosnkowskiego 31, 45-272 Opole, Poland
k.bartecki@po.opole.pl

Abstract: Results of the impulse response analysis for a class of dynamical systems, described by two weakly coupled linear partial differential equations of hyperbolic type, defined on a one-dimensional spatial domain are presented. For the case of two boundary inputs of the Dirichlet type, the analytical expressions for the impulse response functions are derived based on the inverse Laplace transform of the 2×2 transfer function matrix of the system. The influence of the boundary inputs configuration on the impulse response functions is demonstrated. The considerations are illustrated with a practical example of a thin-walled double-pipe heat exchanger operating in parallel- and countercurrent-flow modes, which correspond to the analyzed boundary conditions.

Keywords: hyperbolic system, balance law, transfer function, impulse response, Laplace transform, heat exchanger.

1. Introduction

The concept of the impulse response of a dynamical system is essential in many areas, such as control, economics, electronic processing, electrical and mechanical engineering or acoustic and audio applications (Bonelli and Radzicki, 2008; Kocięcki, 2010; Lee et al., 2007; Wu et al., 2012). For the continuous-time systems, the impulse response can be considered as a response to the input forcing in the form of a Dirac delta distribution. The usefulness of this kind of mathematical representation lies in the fact that it completely characterizes the dynamical properties of the system and can be used to determine its response to arbitrary input signals.

In the case of distributed parameter systems (DPSs), i.e., dynamical systems described by partial differential equations (PDEs), the impulse response function

*Submitted: July 2015; Accepted: September 2015

depends not only on time but also on the spatial variable(s), which represent(s) the geometry of the system. This fact is very important from both practical and technological points of view. The knowledge of the complete spatiotemporal response of the plant allows not only to determine, e.g., the fluid temperature variations at the outlet of a heat exchanger, the pressure variations at the outflow of a transportation pipeline or the voltage at the end point of an electrical transmission line, but also enables the analysis of their distribution along the respective geometrical axis (Baranowski and Mitkowski, 2012; Bartecki, 2009, 2015; Grabowski, 2007; Mitkowski, 2014; Wang et al., 2005). The response of the system to the unit impulse can be interpreted as the Green's function for the given boundary value problem. In some cases, this function can be derived from the first-principle knowledge. On the other hand, when the analytical Green's function is not available, it can be estimated from the input–output data. The first approach is informally known as *white box modeling*, while the second—as *black box modeling*, which obviously relates to the field of system identification (Guo et al., 2010; Li and Qi, 2010; Uciński, 2012).

As is generally known, the notion of the impulse response of a dynamical system is closely related with its transfer function representation. Assuming linearity and time-invariance, the impulse response function $g(t)$ is equal to the inverse Laplace transform of the transfer function $G(s)$. There exists a plethora of literature concerning transfer function modeling and analysis, however, only a few of them take focus on the infinite-dimensional systems. Some of them investigate the transfer functions of DPSs from a strictly mathematical, functional analysis–based viewpoint (see, e.g., Callier and Winkin, 1993; Zwart, 2004), whereas some others to a greater extent take into account the perspective of their practical applications. As an example one can mention, e.g., the article by Rabenstein (1999), in which the concept of the transfer function model has been extended to the DPSs with bounded spatial domains, i.e., systems, which can be described as initial-boundary-value problems. In the tutorial paper by Curtain and Morris (2009), the rich variety of transfer functions for the systems described by PDEs is illustrated by means of several examples under various boundary conditions. Another valuable example is the work by Jacob and Zwart (2012), which concerns the transfer function approach in a general setting of the so-called *Linear Port-Hamiltionian Systems*, where the authors skilfully combine the abstract functional analytical approach with the physical-based modeling.

The current paper tries to fit into the second category, where the analytical results are motivated by the practical examples. It deals with a certain class of DPSs, in which the mass, heat and energy transport phenomena take place. This class of systems, among which one can mention, e.g., heat exchangers, transport pipelines, irrigation channels, or electrical transmission lines, is usually described by PDEs of hyperbolic type and known under the common name of *hyperbolic systems of conservation/balance laws* (Bressan, 1999; Dafermos, 2010; Lax and Wendroff, 1960; Lasiecka and Triggiani, 2008; LeFloch, 2002; Murawski and Lee, 2012; Ziółko, 2000). The present paper can be seen as a continuation of our works (Bartecki 2013 b and c), in which the steady-state properties and the transfer functions of this class of DPSs have been analyzed, respectively. As compared to the two above-mentioned previous papers, the main contribution of the current study concerns the time-domain representation and includes derivation of analytical expressions for the impulse responses of 2×2 hyperbolic systems of balance laws, assuming two different typical configurations of the Dirichlet boundary inputs. The present is organized as follows. Section 2 presents a mathematical model of the considered class of DPSs in the form of PDEs, then recalls its hyperbolicity conditions and transfer function representation. In Section 3, analytical expressions for the impulse responses are derived from the transfer functions of the system, based on the inverse Laplace transform approach. In Section 4, the thin-walled double-pipe heat exchanger, operating in parallel- and countercurrent-flow modes is introduced as a typical example of the hyperbolic DPS with two different boundary input configurations. Next, some of its impulse response functions are presented in the form of two- and three-dimensional plots, representing their spatiotemporal profiles. The paper concludes with Section 5, containing the summary of the presented results.

2. Hyperbolic systems

2.1. Linear PDE representation

Dynamical properties of some of the above-mentioned DPSs can be described, after possible linearization, by the following system of linear homogeneous PDEs of the first order (see Bartecki, 2013b,c; Chentouf and Wang, 2009; Diagne et al., 2012; Evans, 1998; Mattheij et al., 2005):

$$\frac{\partial x\,(l,t)}{\partial t} + \Lambda \frac{\partial x\,(l,t)}{\partial l} = Kx\,(l,t)\,, \tag{1}$$

where $x(l,t) : \Omega \times [0,+\infty) \to \mathbb{R}^n$ is a vector function representing the spatiotemporal distribution of the n state variables

$$x(l,t) = \begin{bmatrix} x_1(l,t) & x_2(l,t) & \ldots & x_n(l,t) \end{bmatrix}^T, \tag{2}$$

with $\Omega = [0,L] \subset \mathbb{R}$ being the domain of the spatial variable l; $[0,+\infty)$ – the domain of the time variable t; $K \in \mathbb{R}^{n\times n}$ – a matrix with constant entries and Λ – a diagonal matrix of the following form:

$$\Lambda = \operatorname{diag}\left(\lambda_1, \ldots, \lambda_p, \lambda_{p+1}, \ldots, \lambda_n\right), \tag{3}$$

with $\lambda_i \in \mathbb{R} \setminus 0$ and

$$\lambda_1 > \ldots > \lambda_p > 0 > \lambda_{p+1} > \ldots > \lambda_n, \tag{4}$$

where $p \leq n$ represents the number of positive elements λ_i.

Definition 1. *The system (1) is said to be* hyperbolic *iff all diagonal entries of Λ, given by (3), are real and different from zero, as assumed in (4). Additionally, if they all are distinct, then the system (1) is said to be* strictly hyperbolic*.*

Definition 2. *The systems, described by (1) with $K \neq 0$, are commonly known as* systems of balance laws*. In the special case when there is no "production", i.e., for $K = 0$, the system is usually called* system of conservation laws *(Dafermos, 2010).*

Remark 1. *Owing to the diagonal form of Λ, each equation of the system (1) contains both temporal and spatial derivatives of the same state variable $x_i(l,t)$, for $i = 1, 2, \ldots, n$. Therefore, this system is commonly referred to as* decoupled *or* weakly coupled*, i.e., coupled only through the terms that do not contain derivatives. In the case of the hyperbolic PDEs, describing physical phenomena mentioned in Section 1, the elements of Λ usually represent the mass and/or energy transport rates.*

Remark 2. *Some of the physical hyperbolic systems are described directly by the weakly coupled PDEs (1), while the others by the* strongly coupled *equations with non-diagonal matrices at the derivative terms. In order to express them in the general form (1), the* decoupling *(diagonalization) procedure has to be carried out (Bartecki, 2013a).*

2.2. Initial and boundary conditions

In order to obtain a unique solution of (1), the appropriate *initial* and *boundary* conditions must usually be specified. The initial conditions represent the initial (i.e., determined for $t = 0$) distribution of the values of all n state variables for the whole set Ω

$$x(l,0) = x_0(l), \tag{5}$$

where $x_0(l) : \Omega \to \mathbb{R}^n$ is a given vector function.

On the other hand, the boundary conditions represent the requirements to be met by the solution $x(l,t)$ at the boundary points of Ω. They can express, e.g., the boundary feedbacks and reflections, as well as the external *boundary inputs* to the system. In general, these conditions may take the form of a linear combination of the Dirichlet and Neumann boundary conditions, as the so-called boundary conditions of the third kind (Ancona and Coclite, 2005; Dooge and Napiorkowski, 1987). The boundary conditions of Dirichlet type, which are often encountered for the considered class of hyperbolic systems, can be written down in the following compact way (Diagne et al., 2012; Xu and Sallet, 2002):

$$\begin{bmatrix} x^+(0,t) \\ x^-(L,t) \end{bmatrix} = \begin{bmatrix} P_{0L} & P_{00} \\ P_{LL} & P_{L0} \end{bmatrix} \begin{bmatrix} x^+(L,t) \\ x^-(0,t) \end{bmatrix} + \begin{bmatrix} R_0 \\ R_L \end{bmatrix} u\,(t) \tag{6}$$

with

$$x^+ = \begin{bmatrix} x_1 & \ldots & x_p \end{bmatrix}^T, \quad x^- = \begin{bmatrix} x_{p+1} & \ldots & x_n \end{bmatrix}^T. \tag{7}$$

The vector function $u(t) : [0, +\infty) \to \mathbb{R}^r$ in (6) expresses the inhomogeneity of the boundary conditions which can be identified with r external inputs to the system, including both control signals and external disturbances. The constant matrices $P_{0L} \in \mathbb{R}^{p\times p}$ and $P_{L0} \in \mathbb{R}^{(n-p)\times(n-p)}$ express the feedbacks from the boundary $l = L$ to the boundary $l = 0$, and from $l = 0$ to $l = L$, respectively. The matrices $P_{00} \in \mathbb{R}^{p\times(n-p)}$ and $P_{LL} \in \mathbb{R}^{(n-p)\times p}$ express the boundary reflections for $l = 0$ and $l = L$, respectively. Finally, $R_0 \in \mathbb{R}^{p\times r}$ and $R_L \in \mathbb{R}^{(n-p)\times r}$ represent the effect of the external inputs $u(t)$ on the boundary conditions $x^+(0, t)$ and $x^-(L, t)$, respectively.

2.3. 2×2 hyperbolic systems

An important class of the considered DPSs is constituted by the systems which can be described, under certain assumptions, by the system of *two* hyperbolic PDEs including *two* main spatiotemporal state variables. The following are some typical examples:

- Thin-walled double-pipe heat exchanger with distributed temperatures $\vartheta_1(l, t)$ and $\vartheta_2(l, t)$ of the heating and the heated fluid (Bartecki, 2015; Grabowski, 2007; Maidi et al., 2010).
- Electrical transmission line with distributed voltage $u(l, t)$ and current $i(l, t)$ (Baranowski and Mitkowski, 2012; Wang et al., 2005).
- Transport pipeline with distributed pressure $p(l, t)$ and flow $q(l, t)$ of the transported medium (Bartecki, 2009).
- Unidirectional open channel flow described by the linearized Saint-Venant equations with the discharge $q(l, t)$ and water depth $h(l, t)$ (Bounit, 2003; Litrico and Fromion, 2009; Strupczewski and Kundzewicz, 1979).

As stated in Remark 2, some of the considered systems, such as the abovementioned heat exchanger, are described directly by the weakly coupled hyperbolic PDEs (1), while the equations of the others are strongly coupled. After possible decoupling, one obtains from (1) for $n = 2$ the following vector of the *characteristic* state variables:

$$x(l, t) = \begin{bmatrix} x_1(l, t) & x_2(l, t) \end{bmatrix}^T, \tag{8}$$

as well as the following matrices of constant coefficients:

$$\Lambda = \begin{bmatrix} \lambda_1 & 0 \\ 0 & \lambda_2 \end{bmatrix}, \quad K = \begin{bmatrix} k_{11} & k_{12} \\ k_{21} & k_{22} \end{bmatrix}. \tag{9}$$

Throughout the rest of the paper we assume, according to Bartecki (2013b and c), that neither boundary feedback nor reflection are present in the system, i.e., $P_{00} = P_{0L} = P_{L0} = P_{LL} = 0$ in (6). Moreover, we consider here two boundary input signals $u_1(t)$ and $u_2(t)$ (i.e., $r = n = 2$) with two different typical input configurations. For the first configuration, both boundary inputs are given for the same edge ($l = 0$) of the spatial domain Ω, whereas for the second one – the input functions $u_1(t)$ and $u_2(t)$ act on the two different edges, $l = 0$ and $l = L$, respectively. Therefore, two definitions are introduced below in order to distinguish between the two above-mentioned configurations.

Definition 3. *The external inputs of the system (1) with $n = 2$ state variables will be referred to as* collocated *Dirichlet boundary inputs, assuming $p = r = 2$ and $R_0 = I_{2\times 2}$ in (6), which for $P_{00} = P_{0L} = P_{L0} = P_{LL} = 0$ leads to the following expression on the boundary input vector:*

$$u^{+}(t) = \begin{bmatrix} u_1^{+}(t) \\ u_2^{+}(t) \end{bmatrix} = \begin{bmatrix} x_1(0,t) \\ x_2(0,t) \end{bmatrix}. \tag{10}$$

Definition 4. *The external inputs of the system (1) with $n = 2$ state variables will be referred to as* anti-collocated *Dirichlet boundary inputs, assuming $r = 2$, $p = 1$ and $R_0 = [1\ 0]$, $R_L = [0\ 1]$ in (6), which for $P_{00} = P_{0L} = P_{L0} = P_{LL} = 0$ leads to the following expression on the boundary input vector:*

$$u^{\pm}(t) = \begin{bmatrix} u_1^{+}(t) \\ u_2^{-}(t) \end{bmatrix} = \begin{bmatrix} x_1(0,t) \\ x_2(L,t) \end{bmatrix}. \tag{11}$$

Remark 3. *Taking into account (4), the collocated inputs will be imposed for $\lambda_1 > 0$ and $\lambda_2 > 0$, while the anti-collocated ones – for $\lambda_1 > 0$ and $\lambda_2 < 0$.*

Furthermore, we take into account in the system two output signals given by the following equation

$$y(t) = \begin{bmatrix} y_1(t) \\ y_2(t) \end{bmatrix} = \begin{bmatrix} x_1(l,t) \\ x_2(l,t) \end{bmatrix}, \tag{12}$$

where $y(t) : [0, +\infty) \to \mathbb{R}^2$, represents the vector of the point-wise observations (measurements) performed for both state variables at the position l.

The above assumptions about the form of the boundary conditions representing the external influences on the system have some practical foundation. For example, in the case of the above-mentioned double-pipe heat exchanger, operating in the so-called *parallel-flow* mode (with $\lambda_1 > 0$ and $\lambda_2 > 0$), the inlet temperatures of the heated and the heating medium are given for the same geometric point of the exchanger. On the other hand, the inlet temperatures of the fluids flowing into the exchanger, operating in the *countercurrent-flow* mode (with $\lambda_1 > 0$ and $\lambda_2 < 0$), are to be specified for its two opposite sides. In turn, the output signals $y_1(t)$ and $y_2(t)$ in (12) can be represented by the outflow temperatures of the fluids, $\vartheta_1(L,t)$ and $\vartheta_2(L,t)$, respectively.

2.4. Transfer functions of 2×2 hyperbolic systems

In this section, the main results of our previous paper, Bartecki (2013b) are recalled. The general closed-form expressions for the individual elements of the

2×2 transfer function matrix are proposed here based on the canonical representation of the hyperbolic system (1), assuming two different configurations of boundary inputs, introduced in Section 2.3. Since the properties of the considered transfer functions have been already thoroughly examined in the above-mentioned paper, we have limited ourselves to presenting below the ready-made expressions, with $y(s)$ and $u(s)$ standing for the Laplace transforms $\mathcal{L}_t$ of $y(t)$ and $u(t)$, respectively.

Proposition 1. *(Bartecki, 2013b). The transfer function matrix of the system (1) for $n = 2$ with the collocated boundary inputs (10) and pointwise outputs (12) has the following form:*

$$G^+(l,s) = \begin{bmatrix} G_{11}^+(l,s) & G_{12}^+(l,s) \\ G_{21}^+(l,s) & G_{22}^+(l,s) \end{bmatrix}, \tag{13}$$

with

$$G_{11}^+(l,s) = \frac{y_1(s)}{u_1^+(s)} = \frac{\phi_1(s)-p_{22}(s)}{\phi_1(s)-\phi_2(s)} \mathrm{e}^{\phi_1(s)l} - \frac{\phi_2(s)-p_{22}(s)}{\phi_1(s)-\phi_2(s)} \mathrm{e}^{\phi_2(s)l}, \tag{14}$$

$$G_{21}^+(l,s) = \frac{y_2(s)}{u_1^+(s)} = \frac{p_{21}}{\phi_1(s)-\phi_2(s)} \left(\mathrm{e}^{\phi_1(s)l} - \mathrm{e}^{\phi_2(s)l}\right), \tag{15}$$

for $u_2^+(s) = 0$, and

$$G_{12}^+(l,s) = \frac{y_1(s)}{u_2^+(s)} = \frac{p_{12}}{\phi_1(s)-\phi_2(s)} \left(\mathrm{e}^{\phi_1(s)l} - \mathrm{e}^{\phi_2(s)l}\right), \tag{16}$$

$$G_{22}^+(l,s) = \frac{y_2(s)}{u_2^+(s)} = \frac{\phi_1(s)-p_{11}(s)}{\phi_1(s)-\phi_2(s)} \mathrm{e}^{\phi_1(s)l} - \frac{\phi_2(s)-p_{11}(s)}{\phi_1(s)-\phi_2(s)} \mathrm{e}^{\phi_2(s)l}, \tag{17}$$

for $u_1^+(s) = 0$, all for zero initial conditions, $x_1(l,0) = x_2(l,0) = 0$, where $p_{11}(s)$, p_{12}, p_{21} and $p_{22}(s)$ are elements of the matrix $P(s)$ of the following form:

$$P(s) = \begin{bmatrix} p_{11}(s) & p_{12} \\ p_{21} & p_{22}(s) \end{bmatrix} = \begin{bmatrix} \dfrac{k_{11}-s}{\lambda_1} & \dfrac{k_{12}}{\lambda_1} \\ \dfrac{k_{21}}{\lambda_2} & \dfrac{k_{22}-s}{\lambda_2} \end{bmatrix}, \tag{18}$$

and $\phi_1(s)$, $\phi_2(s)$ are its eigenvalues

$$\phi_{1,2}(s) = \alpha(s) \pm \beta(s), \tag{19}$$

with

$$\alpha(s) = \frac{1}{2}\left(p_{11}(s) + p_{22}(s)\right) \tag{20}$$

and

$$\beta(s) = \frac{1}{2}\sqrt{\left(p_{11}(s) - p_{22}(s)\right)^2 + 4p_{12}p_{21}}. \tag{21}$$

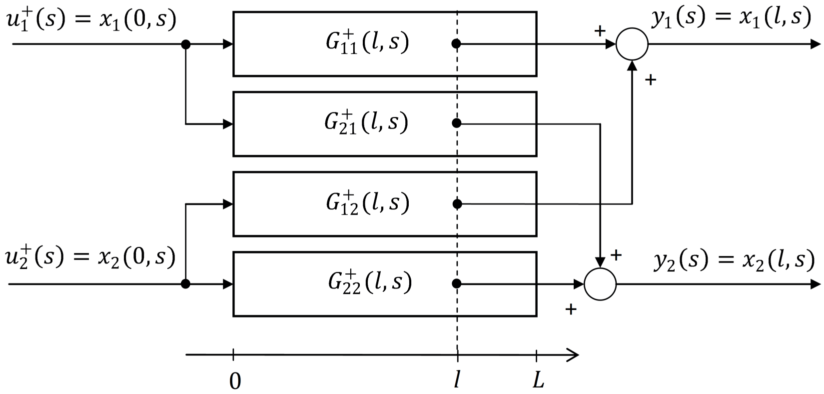

Figure 1. Block diagram of the transfer function model for the collocated boundary inputs

A block diagram of the transfer function model given by Proposition 1 is presented in Fig. 1.

Proposition 2. *(Bartecki, 2013b). For the case of the anti-collocated boundary inputs (11) and pointwise outputs (12) the transfer function matrix of the system (1) for $n = 2$ takes the following form:*

$$G^{\pm}(l,s) = \begin{bmatrix} G_{11}^{\pm}(l,s) & G_{12}^{\pm}(l,s) \\ G_{21}^{\pm}(l,s) & G_{22}^{\pm}(l,s) \end{bmatrix}, \tag{22}$$

where

$$G_{11}^{\pm}(l,s) = \frac{y_1(s)}{u_1^+(s)} = \frac{e^{\phi_2(s)L} e^{\phi_1(s)l} \left(\phi_1(s) - p_{22}(s)\right)}{e^{\phi_2(s)L}(\phi_1(s) - p_{22}(s)) - e^{\phi_1(s)L}(\phi_2(s) - p_{22}(s))} - \frac{e^{\phi_1(s)L} e^{\phi_2(s)l} \left(\phi_2(s) - p_{22}(s)\right)}{e^{\phi_2(s)L}(\phi_1(s) - p_{22}(s)) - e^{\phi_1(s)L}(\phi_2(s) - p_{22}(s))}, \tag{23}$$

$$G_{21}^{\pm}(l,s) = \frac{y_2(s)}{u_1^+(s)} = \frac{p_{21}\left(e^{\phi_2(s)L} e^{\phi_1(s)l} - e^{\phi_1(s)L} e^{\phi_2(s)l}\right)}{e^{\phi_2(s)L}(\phi_1(s) - p_{22}(s)) - e^{\phi_1(s)L}(\phi_2(s) - p_{22}(s))}, \tag{24}$$

for $u_2^-(s) = 0$, and

$$G_{12}^{\pm}(l,s) = \frac{y_1(s)}{u_2^-(s)} = \frac{p_{12}\left(e^{\phi_2(s)l} - e^{\phi_1(s)l}\right)}{e^{\phi_2(s)L}(\phi_2(s) - p_{11}(s)) - e^{\phi_1(s)L}(\phi_1(s) - p_{11}(s))}, \tag{25}$$

$$G_{22}^{\pm}(l,s) = \frac{y_2(s)}{u_2^-(s)} = \frac{e^{\phi_2(s)l}\left(\phi_2(s) - p_{11}(s)\right) - e^{\phi_1(s)l}\left(\phi_1(s) - p_{11}(s)\right)}{e^{\phi_2(s)L}\left(\phi_2(s) - p_{11}(s)\right) - e^{\phi_1(s)L}\left(\phi_1(s) - p_{11}(s)\right)}, \tag{26}$$

for $u_1^+(s) = 0$, *all for zero initial conditions,* $x_1(l,0) = x_2(l,0) = 0$, *where* $p_{11}(s)$, p_{12}, p_{21}, $p_{22}(s)$ *and* $\phi_1(s)$, $\phi_2(s)$ *are given by (18) and (19), respectively.*

A block diagram of the transfer function model given by Proposition 2 is presented in Fig. 2.

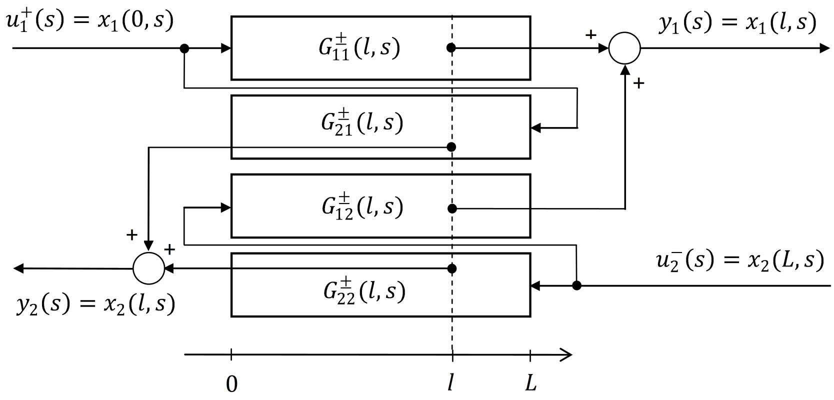

Figure 2. Block diagram of the transfer function model for the anti-collocated boundary inputs

3. Impulse responses

This section presents the main contribution of the paper, which is the general impulse response representation for the 2×2 hyperbolic systems, introduced in Section 2.3. First, definition of the impulse response for the considered class of DPSs with boundary inputs is presented. Next, based on the inverse Laplace transform of the transfer functions discussed in Section 2.4, the analytical expressions describing the impulse response functions are derived, both for the collocated and anti-collocated boundary inputs, adopted in Definitions 3 and 4, respectively.

Definition 5. *Let*

$$G^+(l,t) = \begin{bmatrix} g_{11}^+(l,t) & g_{12}^+(l,t) \\ g_{21}^+(l,t) & g_{22}^+(l,t) \end{bmatrix} \tag{27}$$

and

$$G^{\pm}(l,t) = \begin{bmatrix} g_{11}^{\pm}(l,t) & g_{12}^{\pm}(l,t) \\ g_{21}^{\pm}(l,t) & g_{22}^{\pm}(l,t) \end{bmatrix} \tag{28}$$

represent the impulse response matrices of the system described by the transfer function matrices, given by Proposition 1 and Proposition 2, respectively.

The element $g_{ij}^{+}(l,t)$ *of the matrix given by Eqn. (27) represents the* impulse response *of the channel connecting the* j*th boundary input* $u_j^{+}(t)$*,* $j=1,2$ *from Eqn. (10) with the* i*th pointwise output* $y_i(t)$*,* $i=1,2$ *given by Eqn. (12), i.e., the response due to the Dirac delta boundary condition* $u_j^{+}(t)=x_j(0,t)=\delta(t)$*, assuming zero initial conditions and zero boundary condition for the other input (see Fig. 1).*

Similarly, the elements $g_{ij}^{\pm}(l,t)$ *of the matrix in Eqn. (28) represent the impulse responses of the channels connecting the anti-collocated boundary inputs* $u^{\pm}(t)$ *in Eqn. (11) with the pointwise outputs* $y(t)$ *from Eqn. (12) (see Fig. 2).*

It is well known that the transfer function of a linear time-invariant system is represented by the Laplace transform of its impulse response. Therefore, the impulse response $g_{ij}(l,t)$ given by Definition 5, can be calculated based on the following formula expressing the inverse Laplace transform:

$$g_{ij}\left(l,t\right)=\mathcal{L}_s^{-1}\left\{G_{ij}\left(l,s\right)\right\}=\frac{1}{2\pi i}\lim_{T\to\infty}\int\limits_{\gamma-iT}^{\gamma+iT}e^{st}G_{ij}\left(l,s\right)ds, \tag{29}$$

where $G_{ij}(l,s)$ is the transfer function of the corresponding input–output channel given by (14)–(17) or (23)–(26). The integration in (29) is done along the vertical line Re(s)=γ in the complex plane such that γ is greater than the real part of all singularities of $G_{ij}(l,s)$.

The so-called Bromwich integral, given by (29), provides a very general approach for determining the impulse response of a dynamic system on the basis of its transfer function. The calculations can be facilitated, e.g., by the use of the Cauchy residue theorem. However, for practical reasons, this laborious task can be replaced (when possible) by finding the expressions for the inverse Laplace transforms in look-up tables and using various properties of the Laplace transform (Polyanin and Manzhirov, 1998). Although the transfer functions of the considered hyperbolic systems are given by relatively complex irrational expressions, the latter approach can still be applied in order to obtain analytical formulas for the impulse responses $g_{ij}^{+}(l,t)$ and $g_{ij}^{\pm}(l,t)$, as this will be shown later in this section.

3.1. Fully decoupled system and system of conservation laws

Since the general analytical expressions for the impulse responses of the considered hyperbolic systems with non-zero elements in the matrix K are quite complex as it will be shown later in Subsection 3.2, we will start here with the relatively simple cases of the fully decoupled hyperbolic system ($k_{12}=k_{21}=0$) and the hyperbolic system of conservation laws ($k_{11}=k_{12}=k_{21}=k_{22}=0$).

3.1.1. Collocated boundary inputs

Proposition 3. *The elements of the impulse response matrix $G^{+}(l,t)$ from (27) for the case of the fully decoupled system with $k_{12}=k_{21}=0$ are given by*

$$G^{+}(l,t)=\begin{bmatrix}\kappa_1^{+}(l)\delta\left(t-\tau_1^{+}(l)\right) & 0\\ 0 & \kappa_2^{+}(l)\delta\left(t-\tau_2^{+}(l)\right)\end{bmatrix}, \tag{30}$$

and for the system of conservation laws with $k_{11}=k_{12}=k_{21}=k_{22}=0$ by

$$G^{+}(l,t)=\begin{bmatrix}\delta\left(t-\tau_1^{+}(l)\right) & 0\\ 0 & \delta\left(t-\tau_2^{+}(l)\right)\end{bmatrix}, \tag{31}$$

where

$$\kappa_1^{+}(l)=\mathrm{e}^{\frac{k_{11}}{\lambda_1}l},\quad \kappa_2^{+}(l)=\mathrm{e}^{\frac{k_{22}}{\lambda_2}l}, \tag{32}$$

represent the position-dependent gains, and

$$\tau_1^{+}(l)=\frac{l}{\lambda_1},\quad \tau_2^{+}(l)=\frac{l}{\lambda_2}, \tag{33}$$

are the position-dependent time-delays of the system.

Proof. Assuming $k_{12}=k_{21}=0$ in (9) we obtain the diagonal form of the matrix $P(s)$ in (18) and consequently the following greatly simplified form of the transfer function matrix $G^{+}(l,s)$ from Proposition 1:

$$G^{+}(l,s)=\begin{bmatrix}\mathrm{e}^{\frac{k_{11}-s}{\lambda_1}l} & 0\\ 0 & \mathrm{e}^{\frac{k_{22}-s}{\lambda_2}l}\end{bmatrix}=\begin{bmatrix}\kappa_1^{+}(l)\mathrm{e}^{-s\tau_1^{+}(l)} & 0\\ 0 & \kappa_2^{+}(l)\mathrm{e}^{-s\tau_2^{+}(l)}\end{bmatrix}. \tag{34}$$

The inverse Laplace transform of (34) results in (30).

For the system of conservation laws we obtain $\kappa_1^{+}=\kappa_2^{+}=1$ in (32), which leads to the pure time-delay system with the transfer function matrix

$$G^{+}(l,s)=\begin{bmatrix}\mathrm{e}^{-s\tau_1^{+}(l)} & 0\\ 0 & \mathrm{e}^{-s\tau_2^{+}(l)}\end{bmatrix}, \tag{35}$$

for which the impulse responses take the form given by (31). ■

Remark 4. *The response matrix in (31) contains the Dirac delta impulses "traveling" between $l=0$ and $l=L$ with speeds λ_1 and λ_2. In the case given by (30), the Dirac impulses are additionally scaled by the factor exponentially depending on the spatial position l.*

3.1.2. Anti-collocated boundary inputs

Proposition 4. *The elements of the impulse response matrix $G^{\pm}(l,t)$ from (28) for the case of the fully decoupled system are given by*

$$G^{\pm}(l,t) = \begin{bmatrix} \kappa_1^{+}(l)\delta\left(t-\tau_1^{+}\right) & 0 \\ 0 & \kappa_2^{-}(l)\delta\left(t-\tau_2^{-}\right) \end{bmatrix}, \tag{36}$$

and for the system of conservation laws by

$$G^{\pm}(l,t) = \begin{bmatrix} \delta\left(t-\tau_1^{+}\right) & 0 \\ 0 & \delta\left(t-\tau_2^{-}\right) \end{bmatrix}, \tag{37}$$

where

$$\kappa_1^{+}(l) = \mathrm{e}^{\frac{k_{11}}{\lambda_1}l}, \quad \kappa_2^{-}(l) = \mathrm{e}^{\frac{k_{22}}{\lambda_2}(l-L)}, \tag{38}$$

represent the position-dependent gains and

$$\tau_1^{+}(l) = \frac{l}{\lambda_1}, \quad \tau_2^{-}(l) = \frac{l-L}{\lambda_2}, \tag{39}$$

are the position-dependent time-delays of the system.

Proof. Assuming $k_{12} = k_{21} = 0$ we obtain the following greatly simplified form of the matrix $G^{\pm}(l,s)$ from Proposition 2:

$$G^{\pm}(l,s) = \begin{bmatrix} \kappa_1^{+}(l)\mathrm{e}^{-s\tau_1^{+}(l)} & 0 \\ 0 & \kappa_2^{-}(l)\mathrm{e}^{-s\tau_2^{-}(l)} \end{bmatrix}. \tag{40}$$

The inverse Laplace transform of (40) results in (36).

For the system of conservation laws we obtain $\kappa_1^{+} = \kappa_2^{-} = 1$ in (38) which leads to the pure time-delay system with the transfer function matrix

$$G^{\pm}(l,s) = \begin{bmatrix} \mathrm{e}^{-s\tau_1^{+}(l)} & 0 \\ 0 & \mathrm{e}^{-s\tau_2^{-}(l)} \end{bmatrix}, \tag{41}$$

for which the impulse responses take the form given by (37). ■

3.2. System of balance laws ($K \neq 0$)

For the non-zero elements of the matrix K, representing the case of the system of balance laws (see Definition 2), the calculations are significantly more laborious. Therefore, we will begin by introducing some notations, which will allow for simplifying some complex expressions appearing throughout this subsection.

3.2.1. Preliminary results

Let

$$\eta = 4k_{12}k_{21}\lambda_1\lambda_2, \tag{42}$$

and

$$\gamma(s) = (k_{11} - s)\,\lambda_2 - (k_{22} - s)\,\lambda_1 = \rho s + \sigma, \tag{43}$$

with

$$\rho = \lambda_1 - \lambda_2, \quad \sigma = k_{11}\lambda_2 - k_{22}\lambda_1, \tag{44}$$

where λ_1, λ_2 and k_{11}, k_{12}, k_{21}, k_{22} are elements of the matrices Λ and K in (9).

Lemma 1. *Assuming $\eta \neq 0$, each of the following identities holds:*

$$\gamma(s) + \sqrt{\gamma^2(s) + \eta} = -\frac{\eta}{\gamma(s) - \sqrt{\gamma^2(s) + \eta}}, \tag{45}$$

$$\gamma(s) - \sqrt{\gamma^2(s) + \eta} = -\frac{\eta}{\gamma(s) + \sqrt{\gamma^2(s) + \eta}}. \tag{46}$$

Proof. By dividing each of Eqns. (45) and (46) by their left-hand sides, one obtains the above identities. ■

Lemma 2. *The eigenvalues $\phi_1(s)$ and $\phi_2(s)$ (19) of the matrix $P(s)$ in (18) can be expressed using $\gamma(s)$ from (43) and η from (42) in the following way:*

$$\begin{aligned} \phi_1(s) &= \frac{1}{2\lambda_1\lambda_2}\Big(\gamma(s) + \sqrt{\gamma^2(s) + \eta}\Big) + p_{22}(s) \\ &= -\frac{1}{2\lambda_1\lambda_2}\Big(\gamma(s) - \sqrt{\gamma^2(s) + \eta}\Big) + p_{11}(s), \end{aligned} \tag{47}$$

and

$$\begin{aligned} \phi_2(s) &= \frac{1}{2\lambda_1\lambda_2}\Big(\gamma(s) - \sqrt{\gamma^2(s) + \eta}\Big) + p_{22}(s) \\ &= -\frac{1}{2\lambda_1\lambda_2}\Big(\gamma(s) + \sqrt{\gamma^2(s) + \eta}\Big) + p_{11}(s), \end{aligned} \tag{48}$$

where $p_{11}(s)$ and $p_{22}(s)$ are the diagonal elements of $P(s)$.

Proof. Based on (20) and (43) it is straightforward to show that

$$\alpha(s) = \frac{1}{2\lambda_1\lambda_2}\gamma(s) + p_{22}(s) = -\frac{1}{2\lambda_1\lambda_2}\gamma(s) - p_{11}(s). \tag{49}$$

Similarly, from (21), (42) and (43) one obtains

$$\beta(s) = \frac{1}{2\lambda_1\lambda_2}\sqrt{\gamma^2(s) + \eta}. \tag{50}$$

By combining expressions (19), (49) and (50) one obtains (47) and (48). ■

Remark 5. *Based on (47) and (48), the following relationships can easily be derived:*

$$\phi_1(s) - \phi_2(s) = \frac{1}{\lambda_1 \lambda_2} \sqrt{\gamma^2(s) + \eta}. \tag{51}$$

Lemma 3. *For any $\tau, \mu, \eta, \sigma, \rho \in \mathbb{R}$ such that $\tau \geq 0$, $\eta > 0$, $\rho \neq 0$ and for $n \in \mathbb{N}$, $\gamma(s) \in \mathbb{C}$, the following identity holds:*

$$\begin{aligned} &\mathcal{L}_s^{-1}\left\{ \exp(-s\tau) \frac{\exp\left(\mu\left(\gamma(s) - \sqrt{\gamma^2(s)+\eta}\right)\right)}{\left(\gamma(s)+\sqrt{\gamma^2(s)+\eta}\right)^n \sqrt{\gamma^2(s)+\eta}} \right\} \\ &= H(t-\tau) \exp\left(\frac{\sigma}{\rho}(t-\tau)\right) \left(\frac{t-\tau}{t-\tau+2\mu\rho}\right)^{n/2} \\ &\cdot \frac{\sqrt{\eta}^{-n}}{\rho} J_n\left(\frac{\sqrt{\eta}}{\rho}\sqrt{(t-\tau)(t-\tau+2\mu\rho)}\right), \end{aligned} \tag{52}$$

where $\mathcal{L}_s^{-1}$ represents the inverse Laplace transform in the variable s, H is the Heaviside function given by

$$H(t) = \begin{cases} 0 & for \quad t < 0, \\ 1 & for \quad t \geqslant 0, \end{cases} \tag{53}$$

and J_n denotes the Bessel function of the first kind of order n, i.e. the function given by the following formula:

$$J_n(t) = \sum_{k=0}^{\infty} \frac{(-1)^k}{k!\ \Gamma(k+n+1)} \left(\frac{t}{2}\right)^{2k+n}, \tag{54}$$

with Γ being the gamma function

$$\Gamma(x) = \int_0^{\infty} y^{x-1} e^{-y} dy. \tag{55}$$

Proof (see Friedly, 1975, formulas (9.2-22)-(9.2.24)). By combining the following properties of the inverse Laplace transform:

$$\begin{aligned} &\mathcal{L}_s^{-1}\left\{ \left(\frac{\sqrt{\eta}}{s+\sqrt{s^2+\eta}}\right)^n \frac{\exp\left(\nu\left(s-\sqrt{s^2+\eta}\right)\right)}{\sqrt{s^2+\eta}} \right\} \\ &= \left(\frac{t}{t+2\nu}\right)^{n/2} J_n\left(\sqrt{\eta}\sqrt{t(t+2\nu)}\right), \quad \eta > 0, \end{aligned} \tag{56}$$

$$\mathcal{L}_s^{-1}\{f(\beta s+\alpha)\} = \frac{1}{\beta}\exp\left(-\frac{\alpha t}{\beta}\right) f\left(\frac{t}{\beta}\right), \quad \beta \neq 0, \tag{57}$$

and

$$\mathcal{L}_s^{-1}\left\{\exp\left(-s\tau\right)f\left(s\right)\right\} = H\left(t-\tau\right)f\left(t-\tau\right), \quad \tau \geq 0, \tag{58}$$

where $f(t)$ denotes a given function and $f(s)$ its Laplace transform, one obtains the identity (52). ■

Lemma 4. *For any $\tau, \mu, \eta, \sigma, \rho \in \mathbb{R}$ such that $\tau \geq 0$, $\eta > 0$, $\rho \neq 0$ and for $n \in \mathbb{N}$, $\gamma(s) \in \mathbb{C}$, the following identity holds:*

$$\mathcal{L}_s^{-1}\left\{\exp\left(-s\tau\right)\frac{\exp\left(\mu\left(\gamma(s)-\sqrt{\gamma^2(s)+\eta}\right)\right)}{\left(\gamma(s)+\sqrt{\gamma^2(s)+\eta}\right)^n}\right\}$$

$$= H\left(t-\tau\right)\exp\left(\frac{\sigma}{\rho}\left(t-\tau\right)\right)\frac{1}{t-\tau} \tag{59}$$

$$\left\{\mu\sqrt{\eta}^{-n+1}\left(\frac{t-\tau}{t-\tau+2\mu\rho}\right)^{(n+1)/2} J_{n+1}\left(\frac{\sqrt{\eta}}{\rho}\sqrt{\left(t-\tau\right)\left(t-\tau+2\mu\rho\right)}\right)\right.$$

$$\left.+\,n\sqrt{\eta}^{-n}\left(\frac{t-\tau}{t-\tau+2\mu\rho}\right)^{n/2} J_n\left(\frac{\sqrt{\eta}}{\rho}\sqrt{\left(t-\tau\right)\left(t-\tau+2\mu\rho\right)}\right)\right\}.$$

Proof (see Friedly, 1975, formulas (9.5-6)-(9.5.7)). By combining the following identity:

$$\frac{\exp\left(\mu\left(\gamma-\sqrt{\gamma^2+\eta}\right)\right)}{\left(\gamma+\sqrt{\gamma^2+\eta}\right)^n} = \int_\gamma^\infty \frac{\exp\left(\mu\left(g-\sqrt{g^2+\eta}\right)\right)}{\left(g+\sqrt{g^2+\eta}\right)^n\sqrt{g^2+\eta}}\left(\frac{\mu\eta}{g+\sqrt{g^2+\eta}}+n\right)dg \tag{60}$$

with the well-known property of the Laplace transform

$$\mathcal{L}_s^{-1}\left\{\int_s^\infty f(\sigma)d\sigma\right\} = \frac{1}{t}f(t), \quad s > \alpha, \tag{61}$$

which remains valid for any function $f(t)$ piecewise continuous on $[0, +\infty]$ of exponential order α and such that $\lim_{t\to 0^+} f(t)/t$ exists, and then using Lemma 3, one obtains (59). ■

Remark 6. *For $\eta < 0$, all η appearing on the right-hand sides of (52), (56) and (59) should be replaced with $-\eta$ and the Bessel function of the first kind J_n – with the modified Bessel function of the first kind I_n.*

3.2.2. Collocated boundary inputs

Proposition 5. *The elements of the impulse response matrix* $G^{+}(l,t)$ *from (27) take the following general form:*

$$g^{+}_{ij}(l,t) = \varepsilon^{+}_{ij}\Big\{H\left(t-\tau^{+(1)}(l)\right)\kappa^{+(1)}(l)\chi^{+(1)}_{ij}(l,t) \\ -H\left(t-\tau^{+(2)}(l)\right)\kappa^{+(2)}(l)\chi^{+(2)}_{ij}(l,t)\Big\}, \tag{62}$$

where $i = 1,2$ *and* $j = 1,2$ *represent the output and the input number, respectively, the factor* ε_{ij} *has the following form for the corresponding input–output channels:*

$$\varepsilon^{+}_{11} = \varepsilon^{+}_{22} = -\frac{\sqrt{\eta}}{2\rho}, \quad \varepsilon^{+}_{12} = \frac{k_{12}\lambda_2}{\rho}, \quad \varepsilon^{+}_{21} = \frac{k_{21}\lambda_1}{\rho}, \tag{63}$$

$\tau^{+(1)}(l)$ *and* $\tau^{+(2)}(l)$ *are time delays of the response*

$$\tau^{+(1)}(l) = \frac{l}{\lambda_1}, \quad \tau^{+(2)}(l) = \frac{l}{\lambda_2}, \tag{64}$$

$\kappa^{+(1)}(l)$ *and* $\kappa^{(2)}(l)$ *are functions of the spatial variable* l

$$\kappa^{+(1)}(l) = \exp\left(k_{11}\frac{l}{\lambda_1}\right), \quad \kappa^{+(2)}(l) = \exp\left(k_{22}\frac{l}{\lambda_2}\right), \tag{65}$$

and $\chi^{+(1)}_{ij}(l,t)$, $\chi^{+(2)}_{ij}(l,t)$ *represent the parts of the response, which depend both on the time and the spatial variables:*

$$\chi^{+(m)}_{ij}(l,t) = \exp\left(-\frac{\sigma}{\rho}\left(t-\tau^{+(m)}(l)\right)\right)\left(\frac{t-\tau^{+(1)}(l)}{t-\tau^{+(2)}(l)}\right)^{c} \\ \cdot J_{2|c|}\left(\frac{\sqrt{\eta}}{\rho}\sqrt{\left(t-\tau^{+(1)}(l)\right)\left(t-\tau^{+(2)}(l)\right)}\right), \tag{66}$$

with

$$c = \begin{cases} -\frac{1}{2} & \text{for} \quad i=j=1, \\ 0 & \text{for} \quad i \neq j, \\ \frac{1}{2} & \text{for} \quad i=j=2. \end{cases} \tag{67}$$

Proof. The transfer function $G^{+}_{11}(l,s)$, given by (14), can be transformed, using Lemma 2 and Remark 5, into the following form:

$$G^{+}_{11}(l,s) = \frac{1}{2}\frac{\gamma(s)+\sqrt{\gamma^2(s)+\eta}}{\sqrt{\gamma^2(s)+\eta}} \\ \cdot \exp\left(-\frac{l}{2\lambda_1\lambda_2}\left(\gamma(s)-\sqrt{\gamma^2(s)+\eta}\right)\right)\exp\left(k_{11}\frac{l}{\lambda_1}\right)\exp\left(-\frac{l}{\lambda_1}s\right) \tag{68}$$

$$+\frac{1}{2}\frac{\eta}{\left(\gamma(s)+\sqrt{\gamma^2(s)+\eta}\right)\sqrt{\gamma^2(s)+\eta}}$$
$$\cdot\exp\left(\frac{l}{2\lambda_1\lambda_2}\left(\gamma(s)-\sqrt{\gamma^2(s)+\eta}\right)\right)\exp\left(k_{22}\frac{l}{\lambda_2}\right)\exp\left(-\frac{l}{\lambda_2}s\right).$$

Next, based on Lemma 3, assuming $n=-1$ for the first and $n=1$ for the second term of the transfer function (68), one obtains its inverse Laplace transform in the form expressed by (62) for $i=j=1$.

Similarly, the transfer function $G_{12}^{+}(l,s)$ from (16) can be expanded as follows:

$$G_{12}^{+}(l,s)=\frac{k_{12}\lambda_2}{\sqrt{\gamma^2(s)+\eta}} \tag{69}$$
$$\cdot\left\{\exp\left(-\frac{l}{2\lambda_1\lambda_2}\left(\gamma(s)-\sqrt{\gamma^2(s)+\eta}\right)\right)\exp\left(k_{11}\frac{l}{\lambda_1}\right)\exp\left(-\frac{l}{\lambda_1}s\right)\right.$$
$$\left.-\exp\left(\frac{l}{2\lambda_1\lambda_2}\left(\gamma(s)-\sqrt{\gamma^2(s)+\eta}\right)\right)\exp\left(k_{22}\frac{l}{\lambda_2}\right)\exp\left(-\frac{l}{\lambda_2}s\right)\right\}.$$

Then, the use of Lemma 3 for $n=0$ results in the inverse Laplace transform of (69), representing the impulse response (62) for $i=1$ and $j=2$. Due to the symmetry, one can obtain impulse responses $g_{21}^{+}(l,t)$ and $g_{22}^{+}(l,t)$ from the transfer functions (15) and (17) in a similar manner. ■

3.2.3. Anti-collocated boundary inputs

PROPOSITION 6. *The elements of the impulse response matrix $G^{\pm}(l,t)$ from (28) take the following general form:*

$$g_{ij}^{\pm}(l,t)=\varepsilon_{ij}^{\pm}\sum_{m=0}^{\infty}\left\{H\left(t-\tau_{j,m}^{\pm(1)}(l)\right)\kappa_{j,m}^{\pm(1)}(l)\,\chi_{ij,m}^{\pm(1)}(l,t)\right.$$
$$\left.-H\left(t-\tau_{j,m}^{\pm(2)}(l)\right)\kappa_{j,m}^{\pm(2)}(l)\,\chi_{ij,m}^{\pm(2)}(l,t)\right\}, \tag{70}$$

where the kth term of the infinite series represents the number of the wave appearing in the response, $i=1,2$ and $j=1,2$ are the output and the input number, respectively, the values of $\varepsilon_{ij}^{\pm}$ are given as follows:

$$\varepsilon_{11}^{\pm}=\varepsilon_{22}^{\pm}=1,\quad \varepsilon_{12}^{\pm}=-\frac{2k_{12}\lambda_2}{\sqrt{-\eta}},\quad \varepsilon_{21}^{\pm}=\frac{2k_{21}\lambda_1}{\sqrt{-\eta}}, \tag{71}$$

$\tau_{j,m}^{\pm(1)}(l)$ *and* $\tau_{j,m}^{\pm(2)}(l)$ *are time delays for the* m*th wave and the* j*th input equal to*

$$\begin{aligned} \tau_{1,k}^{\pm(1)}(l) &= \frac{kL+l}{\lambda_1} - \frac{kL}{\lambda_2}, & \tau_{1,k}^{\pm(2)}(l) &= \frac{(k+1)L}{\lambda_1} - \frac{(k+1)L-l}{\lambda_2}, \\ \tau_{2,k}^{\pm(1)}(l) &= \frac{kL}{\lambda_1} - \frac{(k+1)L-l}{\lambda_2}, & \tau_{2,k}^{\pm(2)}(l) &= \frac{kL+l}{\lambda_1} - \frac{(k+1)L}{\lambda_2}, \end{aligned} \tag{72}$$

$\kappa_{j,k}^{\pm(1)}(l)$ *and* $\kappa_{j,k}^{\pm(2)}(l)$ *are functions of the spatial variable* l

$$\begin{aligned} \kappa_{1,k}^{\pm(1)}(l) &= \exp\left(k_{11}\frac{kL+l}{\lambda_1} - k_{22}\frac{kL}{\lambda_2}\right), \\ \kappa_{1,k}^{\pm(2)}(l) &= \exp\left(k_{11}\frac{(k+1)L}{\lambda_1} - k_{22}\frac{(k+1)L-l}{\lambda_2}\right), \\ \kappa_{2,k}^{\pm(1)}(l) &= \exp\left(k_{11}\frac{kL}{\lambda_1} - k_{22}\frac{(k+1)L-l}{\lambda_2}\right), \\ \kappa_{2,k}^{\pm(2)}(l) &= \exp\left(k_{11}\frac{kL+l}{\lambda_1} - k_{22}\frac{(k+1)L}{\lambda_2}\right), \end{aligned} \tag{73}$$

and $\chi_{ij,k}^{\pm(1)}(l,t)$, $\chi_{ij,k}^{\pm(2)}(l,t)$ *represent the parts of the response, which depend both on the time and the spatial variable:*

$$\begin{aligned} \chi_{ij,k}^{\pm(m)}(l,t) = {} & \frac{1}{t-\tau_{j,k}^{\pm(m)}(l)} \exp\left(-\frac{\sigma}{\rho}\left(t-\tau_{j,k}^{\pm(m)}(l)\right)\right) \\ & \left\{ \mu_{j,k}^{\pm(m)}(l)\sqrt{-\eta}\left(\frac{t-\tau_{j,k}^{\pm(m)}(l)}{t-\tau_{j,k}^{\pm(m)}(l)+2\mu_{j,k}^{\pm(m)}(l)\rho}\right)^{c+\frac{1}{2}} \right. \\ & \cdot I_{2c+1}\left(\frac{\sqrt{-\eta}}{\rho}\sqrt{\left(t-\tau_{j,k}^{\pm(m)}(l)\right)\left(t-\tau_{j,k}^{\pm(m)}(l)+2\mu_{j,k}^{\pm(m)}(l)\rho\right)}\right) \\ & + 2c\left(\frac{t-\tau_{j,k}^{\pm(m)}(l)}{t-\tau_{j,k}^{\pm(m)}(l)+2\mu_{j,k}^{\pm(m)}(l)\rho}\right)^{c} \\ & \left. \cdot I_{2c}\left(\frac{\sqrt{-\eta}}{\rho}\sqrt{\left(t-\tau_{j,k}^{\pm(m)}(l)\right)\left(t-\tau_{j,k}^{\pm(m)}(l)+2\mu_{j,k}^{\pm(m)}(l)\rho\right)}\right) \right\}, \end{aligned} \tag{74}$$

where $m = 1, 2$,

$$c = \begin{cases} k+m-1 & \text{for} \quad i = j, \\ k+\frac{1}{2} & \text{for} \quad i \neq j, \end{cases} \tag{75}$$

and

$$\mu_{1,k}^{\pm(1)}(l) = -\frac{2kL+l}{2\lambda_1\lambda_2}, \qquad \mu_{1,k}^{\pm(2)}(l) = -\frac{2\,(k+1)\,L-l}{2\lambda_1\lambda_2},$$
$$\mu_{2,k}^{\pm(1)}(l) = -\frac{(2k+1)\,L-l}{2\lambda_1\lambda_2}, \quad \mu_{2,k}^{\pm(2)}(l) = -\frac{2\,(k+1)\,L+l}{2\lambda_1\lambda_2}. \tag{76}$$

Proof. After dividing both the numerator and the denominator of the transfer function $G_{11}^{\pm}(l,s)$ in (23) by the expression $\exp(\phi_2(s)L)(\phi_1(s) - p_{22}(s))$ and then using Lemmas 1 and 2 together with Remark 5, one obtains:

$$\begin{aligned} G_{11}^{\pm}(l,s) = {} & \exp\left(-\frac{l}{2\lambda_1\lambda_2}\left(\gamma(s)-\sqrt{\gamma^2(s)+\eta}\right)\right)\exp\left(k_{11}\frac{l}{\lambda_1}\right)\exp\left(-\frac{l}{\lambda_1}s\right) \\ & \cdot\left(1+\exp\left(\frac{L-l}{\lambda_1\lambda_2}\sqrt{\gamma^2(s)+\eta}\right)\frac{\eta}{\left(\gamma(s)+\sqrt{\gamma^2(s)+\eta}\right)^2}\right) \\ & \cdot\left(1+\exp\left(\frac{L}{\lambda_1\lambda_2}\sqrt{\gamma^2(s)+\eta}\right)\frac{\eta}{\left(\gamma(s)+\sqrt{\gamma^2(s)+\eta}\right)^2}\right)^{-1}. \end{aligned} \tag{77}$$

Since we assume boundedness of the considered transfer function and, moreover, we have $L > 0$, $\lambda_1 > 0$ and $\lambda_2 < 0$, we can express the denominator (i.e., the last factor) of (77) in the form of a convergent infinite series:

$$\begin{aligned} & \left(1-\exp\left(\frac{L}{\lambda_1\lambda_2}\sqrt{\gamma^2(s)+\eta}\right)\frac{-\eta}{\left(\gamma(s)+\sqrt{\gamma^2(s)+\eta}\right)^2}\right)^{-1} = \\ & = \sum_{k=0}^{\infty}\left(\frac{-\eta}{\left(\gamma(s)+\sqrt{\gamma^2(s)+\eta}\right)^2}\right)^k \exp\left(\frac{kL}{\lambda_1\lambda_2}\sqrt{\gamma^2(s)+\eta}\right) = \\ & = \sum_{k=0}^{\infty}\left(\frac{-\eta}{\left(\gamma(s)+\sqrt{\gamma^2(s)+\eta}\right)^2}\right)^k \\ & \quad \cdot\exp\left(-\frac{kL}{\lambda_1\lambda_2}\left(\gamma(s)-\sqrt{\gamma^2(s)+\eta}\right)\right)\exp\left(k\frac{\rho L}{\lambda_1\lambda_2}s\right)\exp\left(k\frac{\sigma L}{\lambda_1\lambda_2}\right). \end{aligned} \tag{78}$$

By multiplying the series in (78) by the numerator of the transfer function (77) one obtains

$$G_{11}^{\pm}(l,s) = \sum_{k=0}^{\infty} \Bigg\{ \kappa_{1,k}^{\pm(1)}(l) \exp\left(-s\tau_{1,k}^{\pm(1)}(l)\right) \left(\frac{-\eta}{\left(\gamma + \sqrt{\gamma^2+\eta}\right)^2} \right)^k$$

$$\exp\left(\mu_{1,k}^{\pm(1)}(l)\left(\gamma(s) - \sqrt{\gamma^2(s)+\eta}\right)\right) \tag{79}$$

$$- \kappa_{1,k}^{\pm(2)}(l) \exp\left(-s\tau_{1,k}^{\pm(2)}(l)\right) \left(\frac{-\eta}{\left(\gamma(s) + \sqrt{\gamma^2(s)+\eta}\right)^2} \right)^{k+1}$$

$$\exp\left(\mu_{1,k}^{\pm(2)}(l)\left(\gamma(s) - \sqrt{\gamma^2(s)+\eta}\right)\right) \Bigg\},$$

where $\tau_{j,k}^{\pm(m)}(l)$, $\kappa_{j,k}^{\pm(m)}(l)$ and $\mu_{j,k}^{\pm(m)}(l)$ are given by (72), (73) and (76), respectively. Then, based on Lemma 4 we can take the inverse Laplace transforms of the series in (79) term by term, obtaining, as a result, the impulse response $g_{11}^{\pm}(l,t)$ in the form given by (70). For the remaining transfer functions, the procedure can be performed in a similar way, resulting in the corresponding impulse responses. ■

4. Examples

For a practical illustration of the above-discussed theoretical framework, this section performs impulse response analysis of a thin-walled double-pipe heat exchanger, which can be considered as a typical DPS, whose mathematical description takes the form of the equation (1) with $n = 2$ state variables representing spatiotemporal distribution of the fluid temperatures. The study includes both the exchanger operating in the parallel-flow mode, for which the boundary inputs have the collocated form, specified in the Definition 3, and the countercurrent-flow mode, which corresponds to the anti-collocated boundary inputs, adopted in Definition 4. After having obtained, based on equations (14)–(17) and (23)–(26), the transfer functions of the exchanger, selected impulse responses for the parallel- and countercurrent-flow modes are presented, both in the form of three-dimensional graphs and as classical two-dimensional plots, determined for a given spatial position.

4.1. Parallel-flow heat exchanger

Under some simplifying assumptions, the dynamic properties of the double-pipe heat exchanger with negligible thermal capacitance of the wall can be described, based on the thermal energy balance equations, by the following hyperbolic PDEs (Bagui et al., 2004; Bartecki, 2015; Maidi et al., 2010):

$$\frac{\partial\vartheta_1(l,t)}{\partial t}+v_1\frac{\partial\vartheta_1(l,t)}{\partial l}=\alpha_1\big(\vartheta_2(l,t)-\vartheta_1(l,t)\big), \tag{80}$$

$$\frac{\partial\vartheta_2(l,t)}{\partial t}+v_2\frac{\partial\vartheta_2(l,t)}{\partial l}=\alpha_2\big(\vartheta_1(l,t)-\vartheta_2(l,t)\big), \tag{81}$$

where the 1- and 2- sub-indexed figures represent tube-side and shell-side fluid variables/coefficients, respectively; specifically: $\vartheta_1(l,t)$ and $\vartheta_2(l,t)$ – temperatures, v_1 and v_2 – velocities, α_1 and α_2 – generalized parameters including: heat transfer coefficients, fluid densities, specific heats, and geometric dimensions of the exchanger.

Upon comparing (80) and (81) with the general equation (1), one obtains the following vector of the state variables:

$$x(l,t)=\big[\vartheta_1(l,t) \quad \vartheta_2(l,t)\big]^T. \tag{82}$$

Assuming the following parameter values: $v_1 = 1\ \mathrm{m}\cdot\mathrm{s}^{-1}, v_2 = 0.5\ \mathrm{m}\cdot\mathrm{s}^{-1}$, $\alpha_1 = \alpha_2 = 0.5\ \mathrm{s}^{-1}$, one obtains the following matrices of the system (1):

$$\Lambda=\begin{bmatrix}1 & 0\\ 0 & 0.5\end{bmatrix}, \quad K=\begin{bmatrix}-0.5 & 0.5\\ 0.5 & -0.5\end{bmatrix}, \tag{83}$$

with $\lambda_1 = v_1 = 1$, $\lambda_2 = v_2 = 0.5$ being the characteristic speeds and K symmetric and negative definite, which makes the system dissipative.

The fluid inlet temperatures ϑ_{1i}, ϑ_{2i} can be taken as the input signals, which, in the considered case of the parallel-flow, corresponds to the following collocated boundary inputs (see Definition 3):

$$u^+(t)=\begin{bmatrix}u_1^+(t)\\ u_2^+(t)\end{bmatrix}=\begin{bmatrix}\vartheta_{1i}^+(t)\\ \vartheta_{2i}^+(t)\end{bmatrix}=\begin{bmatrix}\vartheta_1(0,t)\\ \vartheta_2(0,t)\end{bmatrix}. \tag{84}$$

The transfer functions of the heat exchanger are given directly by the equations (14)–(17) and represent the ratio of the Laplace transform of the fluid temperature at the given point l to the Laplace transform of the fluid temperature in the inlet section ($l = 0$) of the exchanger:

$$\vartheta_1(l,s)=G_{11}^+(l,s)\vartheta_{1i}^+(s)+G_{12}^+(l,s)\vartheta_{2i}^+(s), \tag{85}$$

$$\vartheta_2(l,s)=G_{21}^+(l,s)\vartheta_{1i}^+(s)+G_{22}^+(l,s)\vartheta_{2i}^+(s), \tag{86}$$

where $\vartheta(l,s)=\mathcal{L}_t\{\vartheta(l,t)\}$ is the Laplace transform of the function representing the fluid temperature.

Based on the results presented in Section 3.2.2, it is possible to calculate the impulse responses of the exchanger for the above-mentioned flow configuration.

From the practical point of view, these responses represent the spatiotemporal temperature profiles of both fluids involved in the heat exchange caused by the impulse temperature change of one of the fluids at the exchanger inlet (see Definition 5). For the sake of brevity, later in this section we only present the results obtained for one of the input–output channels, represented by the transfer function $G_{21}^{+}(l,s)$.

Figure 3 shows the three-dimensional graph of the impulse response $g_{21}^{+}(l,t)$ determined on the basis of Proposition 5 for the assumed parameter values (83). Next, Figs. 4 and 5 show classical, two-dimensional plots of $g_{21}^{+}(t)$. The first one shows the temperature changes over time, evaluated for $l = 3$, assuming three different parameter configurations. One can observe here the influence of the parameters, such as fluid velocity or heat transfer coefficient, on the overall shape of the response. On the other hand, Fig. 5 displays three impulse responses for the same parameter values, evaluated at three different spatial positions: $l = 0.5$, $l = 2.5$ and $l = 4.5$. It can be easily noticed that this graph contains three different cross-sections of the spatiotemporal plot of Fig. 3.

As seen from the plots, the solution contains jump discontinuities, which can evolve even from smooth initial data. This behavior is typical for hyperbolic systems of balance laws (see Bressan, 1999; Evans, 1998; Mattheij et al., 2005). The plots of the impulse responses for the other input–output channels of the heat exchanger can be obtained in a similar way on the basis of the results presented in Section 3.2.2.

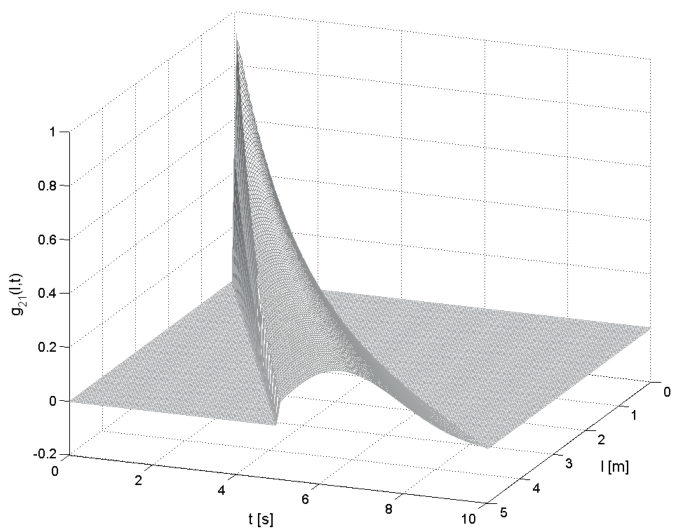

Figure 3. Impulse response $g_{21}^{+}(l,t)$ of the parallel-flow heat exchanger

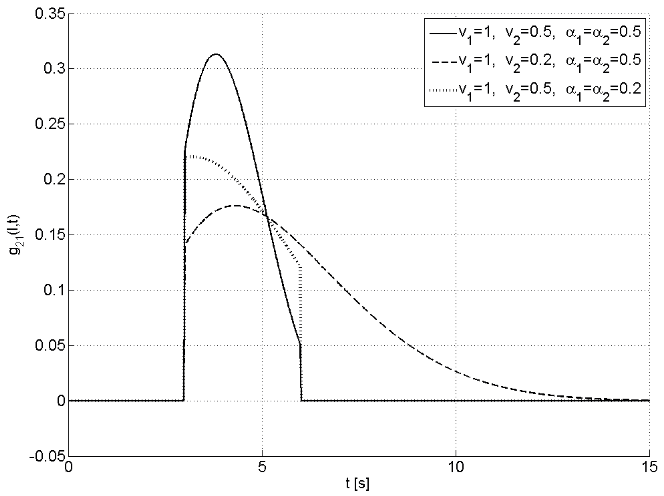

Figure 4. Impulse responses $g_{21}^{+}(t)$ of the parallel-flow heat exchanger for $l = 3$

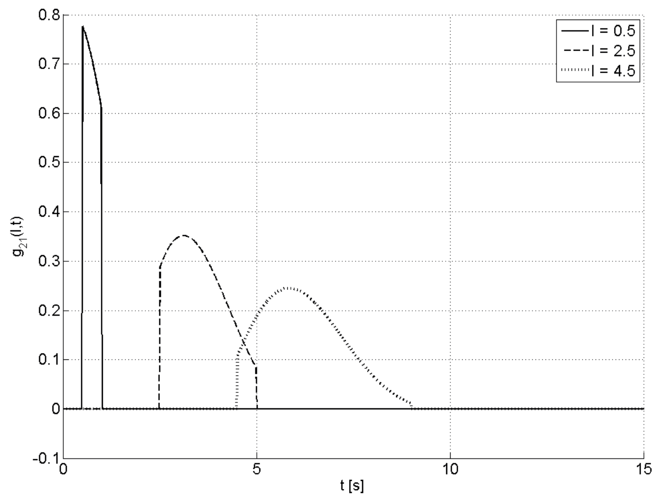

Figure 5. Impulse response $g_{21}^{+}(t)$ of the parallel-flow heat exchanger for $v_1 = 1$, $v_2 = 0.5$ and $\alpha_1 = \alpha_2 = 0.5$

4.2. Countercurrent-flow heat exchanger

For the exchanger operated in the countercurrent mode, the fluids involved in the heat exchange enter the plant from its opposite ends. The PDEs describing the dynamics of the exchanger, have the same form (80)–(81) as for the parallel-flow configuration, and the difference in the mathematical description consists in the opposite signs of fluid velocities ($v_1 > 0$ and $v_2 < 0$), as well as in different boundary conditions. The transfer functions of the heat exchanger are given now by the equations (23)–(26) and describe the following input–output model:

$$\vartheta_1(l,s) = G_{11}^{\pm}(l,s)\vartheta_{1i}^{+}(s) + G_{12}^{\pm}(l,s)\vartheta_{2i}^{-}(s), \tag{87}$$

$$\vartheta_2(l,s) = G_{21}^{\pm}(l,s)\vartheta_{1i}^{+}(s) + G_{22}^{\pm}(l,s)\vartheta_{2i}^{-}(s), \tag{88}$$

with the anti-collocated boundary inputs (see Definition 4):

$$u^{\pm}(t) = \begin{bmatrix} u_1^{+}(t) \\ u_2^{-}(t) \end{bmatrix} = \begin{bmatrix} \vartheta_{1i}^{+}(t) \\ \vartheta_{2i}^{-}(t) \end{bmatrix} = \begin{bmatrix} \vartheta_1(0,t) \\ \vartheta_2(L,t) \end{bmatrix}. \tag{89}$$

The impulse responses of the heat exchanger for the above input configuration have been evaluated based on the results presented in Section 3.2.3. Figure 6 shows the three-dimensional graph of the impulse response $g_{21}^{\pm}(l,t)$, obtained on the basis of Proposition 6 for $v_1 = 1\ \mathrm{m}\cdot\mathrm{s}^{-1}$, $v_2 = -0.5\ \mathrm{m}\cdot\mathrm{s}^{-1}$ and $\alpha_1 = \alpha_2 = 0.2\ \mathrm{s}^{-1}$. As in the case of the parallel-flow configuration, the two subsequent figures show classical, two-dimensional plots for the same input–output channel.

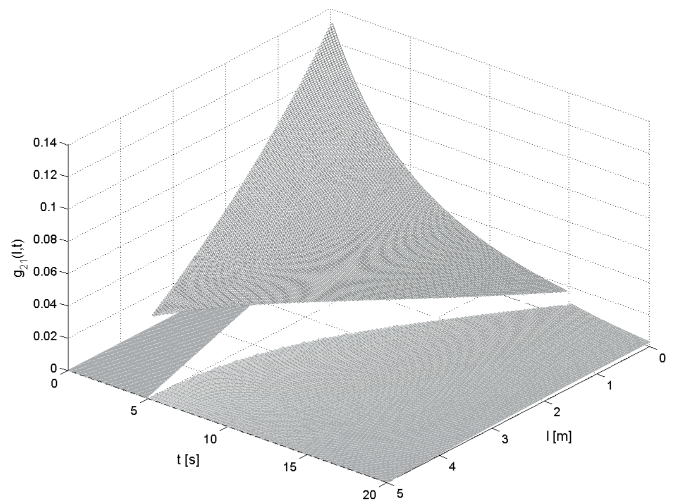

Figure 6. Impulse response $g_{21}^{\pm}(l,t)$ of the countercurrent-flow heat exchanger

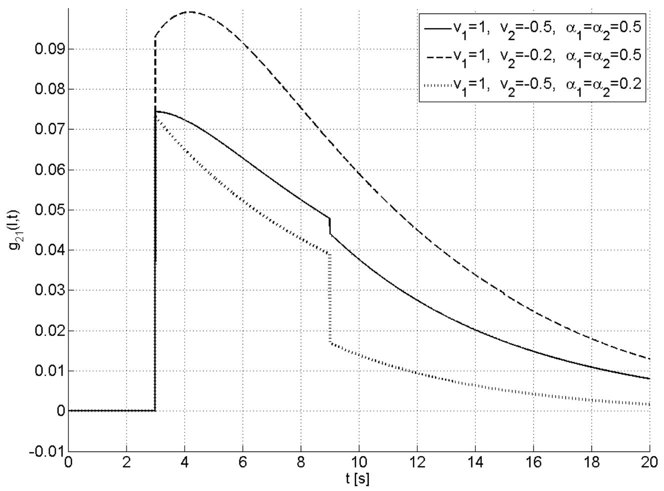

Figure 7. Impulse responses $g_{21}^{\pm}(t)$ of the countercurrent-flow heat exchanger for $l = 3$

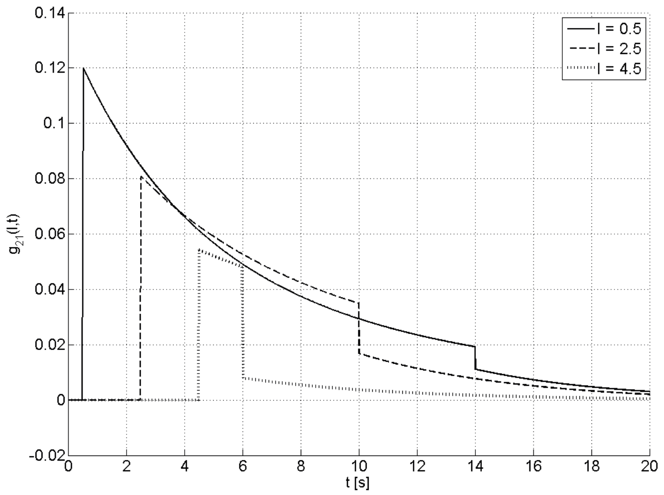

Figure 8. Impulse response $g_{21}^{\pm}(t)$ of the countercurrent-flow heat exchanger for $v_1 = 1$, $v_2 = -0.5$ and $\alpha_1 = \alpha_2 = 0.5$

Figure 7 shows the plots of the impulse responses $g_{21}^{\pm}(t)$, evaluated for $l = 3$ assuming three different parameter configurations given in the figure legend. Figure 8 displays impulse responses evaluated at three different spatial positions:

$l = 0.5$, $l = 2.5$ and $l = 4.5$, which can be considered as three "spatial snapshots" of Fig. 6.

The spatiotemporal impulse responses of the double-pipe heat exchanger, presented here, are consistent with the existing ones, obtained on the basis of both analytical and numerical solutions (see Jaswon, 1954; Gvozdenac, 1990). Since it is impossible to obtain the input signal in the form of the Dirac delta function in the case of the real plant, the here presented results might appear at first sight of little use from the practical point of view. However, as mentioned in Section 1, it is possible to calculate the plant response to an arbitrary input signal by convolving this signal with the impulse response of the system. For example, the unit step responses, commonly used as test inputs for many real plants, can be obtained directly by integration of the impulse responses.

5. Summary

The paper has addressed the problem of the impulse response representation for a class of distributed parameter systems of hyperbolic type with Dirichlet boundary inputs and pointwise outputs/observations. The results presented here can be regarded as a continuation of the analysis performed in Bartecki (2013b), which has been related to the transfer function representation of the considered class of dynamical systems. The analytical expressions for the impulse response functions have been derived based on the inverse Laplace transform of the transfer functions. The influence of the boundary inputs configuration on the form of the impulse responses, which can be identified with the Green's function of the system, has been also demonstrated.

The considerations have been illustrated with the example of a double-pipe heat exchanger operating in parallel- and countercurrent-flow modes, corresponding to the two different boundary inputs configurations. The impulse response functions have been presented both in the form of the three-dimensional graphs, taking into account the spatiotemporal dynamics of the system, as well as the classical two-dimensional plots obtained for a fixed value of the spatial variable, representing the system output. As shown in the paper, the spatiotemporal dynamics of the considered class of systems significantly affects the form of their impulse response functions. As concluded in Bartecki (2013b), their irrational transfer functions manifest some peculiarities, which do not appear in the rational-form case, such as, e.g., fractional order or infinite number of poles and/or zeros. Consequently, the impulse responses, considered here, are described by the relatively complex formulas containing infinite series such as Bessel special functions, which additionally depend on the boundary input configuration.

References

Ancona, F. and Coclite, G. M. (2005) On the boundary controllability of first-order hyperbolic systems. *Nonlinear Analysis: Theory, Methods &*

Applications, **63**(5-7), e1955–e1966.
BAGUI, F., ABDELGHANI-IDRISSI, M.A. and CHAFOUK, H. (2004) Heat exchanger Kalman filtering with process dynamic acknowledgement. *Computers & Chemical Engineering*, **28**(8), 1465–1473.
BARANOWSKI, J. and MITKOWSKI, W. (2012) Stabilisation of LC ladder network with the help of delayed output feedback. *Control and Cybernetics*, **41**(1), 13–34.
BARTECKI, K. (2009) Frequency- and time-domain analysis of a simple pipeline system. In: *Proceedings of the 14th IEEE IFAC International Conference on Methods and Models in Automation and Robotics*. IFAC, www.ifac-papersonline.net/Detailed/41106.html, 366–371.
BARTECKI, K. (2013a) Computation of transfer function matrices for 2×2 strongly coupled hyperbolic systems of balance laws. In: *Proceedings of the 2nd Conference on Control and Fault-Tolerant Systems*. IEEE, http://ieeexplore.ieee.org/stamp/stamp.jsp?tp=&arnumber=6693813, 578–583.
BARTECKI, K. (2013b) A general transfer function representation for a class of hyperbolic distributed parameter systems. *International Journal of Applied Mathematics and Computer Science*, **23**(2), 291–307.
BARTECKI, K. (2013c) Steady-state analysis for a class of hyperbolic systems with boundary inputs. *Archives of Control Sciences*, **23**(3), 295–310.
BARTECKI, K. (2015) Transfer function–based analysis of the frequency-domain properties of a double pipe heat exchanger. *Heat and Mass Transfer*, **51**(2), 277–287.
BONELLI, S. and RADZICKI, K. (2008) Impulse response function analysis of pore pressures in earthdams. *European Journal of Environmental and Civil Engineering*, **12**(3), 243–262.
BOUNIT, H. (2003) The stability of an irrigation canal system. *International Journal of Applied Mathematics and Computer Science*, **13**(4), 453–468.
BRESSAN, A. (1999) Hyperbolic systems of conservation laws. *Revista Matemática Complutense*, **12**(1), 135–200.
CALLIER, F. M. and WINKIN, J. (1993) Infinite dimensional system transfer functions. In: CURTAIN, BENSOUSSAN, LIONS, (eds), *Analysis and Optimization of Systems: State and Frequency Domain Approaches for Infinite-Dimensional Systems*. Lecture Notes in Control and Information Sciences, **185**. Springer, Berlin – Heidelberg.
CHENTOUF, B. and WANG, J. M. (2009) Boundary feedback stabilization and Riesz basis property of a 1-d first order hyperbolic linear system with L^∞-coefficients. *Journal of Differential Equations*, **246**(3), 1119–1138.
CURTAIN, R. and MORRIS, K. (2009) Transfer functions of distributed parameters systems: A tutorial. *Automatica*, **45**(5), 1101–1116.
DAFERMOS, C. M. (2010) *Hyperbolic Conservation Laws in Continuum Physics*. Comprehensive Studies in Mathematics. Springer, Berlin – Heidelberg.
DIAGNE, A., BASTIN, G. and CORON, J.-M. (2012) Lyapunov exponential stability of 1-D linear hyperbolic systems of balance laws. *Automatica*, **48**(1),

109–114.

Dooge, J. C. I. and Napiorkowski, J. J. (1987) The Effect of the Downstream Boundary Conditions in the Linearized St Venant Equations. *The Quarterly Journal of Mechanics and Applied Mathematics*, **40**(2), 245–256.

Evans, L. C. (1998) *Partial Differential Equations.* American Mathematical Society, Providence, USA.

Friedly, J. C. (1975) *Dynamic Behaviour of Processes (Polish edition).* Wydawnictwa Naukowo-Techniczne, Warszawa.

Grabowski, P. (2007) Stability of a heat exchanger feedback control system using the circle criterion. *International Journal of Control*, **80**(9), 1388–1403.

Guo, L.Z., Billings, S. A. and Coca, D. (2010) Identification of partial differential equation models for a class of multiscale spatio-temporal dynamical systems. *International Journal of Control*, **83**(1), 40–48.

Gvozdenac, D. D. (1990) Transient response of the parallel flow heat exchanger with finite wall capacitance. *Archive of Applied Mechanics*, **60**(7), 481–490.

Jacob, B. and Zwart, H. J. (2012) *Linear Port-Hamiltonian Systems on Infinite-dimensional Spaces.* Operator Theory: Advances and Applications, **223**. Springer, Basel.

Jaswon, M.A. (1954) Countercurrent transfer processes in the non-steady state. *Proceedings of the Royal Society of London. Series A, Mathematical and Physical Sciences*, **225**(1161), 226–244.

Kocięcki, A. (2010) A Prior for Impulse Responses in Bayesian Structural VAR Models. *Journal of Business & Economic Statistics*, **28**(1), 115–127.

Lasiecka, I. and Triggiani, R. (2008) Uniform energy decay rates of hyperbolic equations with nonlinear boundary and interior dissipation. *Control and Cybernetics*, **37**(4), 935–969.

Lax, P. and Wendroff, B. (1960) Systems of Conservation Laws. *Communications on Pure and Applied Mathematics*, **13**(2), 217–237.

Lee, P. J., Vítkovský, J. P., Lambert, M. F., Simpson, A. R. and Liggett, J. (2007) Leak location in pipelines using the impulse response function. *Journal of Hydraulic Research*, **45**(5), 643–652.

LeFloch, P. G. (2002) *Hyperbolic Systems of Conservation Laws.* Birkhäuser, Basel.

Li, H.-X. and Qi, C. (2010) Modeling of distributed parameter systems for applications – A synthesized review from time-space separation. *Journal of Process Control*, **20**(8), 891–901.

Litrico, X. and Fromion, V. (2009) *Modeling and Control of Hydrosystems.* Springer, London.

Maidi, A., Diaf, M. and Corriou, J.-P. (2010) Boundary control of a parallel-flow heat exchanger by input–output linearization. *Journal of Process Control*, **20**(10), 1161–1174.

Mattheij, R. M. M., Rienstra, S. W. and ten Thije Boonkkamp, J. H. M. (2005) *Partial Differential Equations: modeling, analysis, computation.* Society for Industrial and Applied Mathematics, (SIAM), Philadelphia.

Mitkowski, W. (2014) Finite-dimensional approximations of distributed RC networks. *Bulletin of the Polish Academy of Sciences: Technical Sciences*, **62**(2), 263–269.

Murawski, K. and Lee, D. (2012) Godunov-type algorithms for numerical modeling of solar plasma. *Control and Cybernetics*, **41**(1), 35–56.

Polyanin, A. D. and Manzhirov, A. V. (1998) *Handbook of Integral Equations.* CRC Press, Boca Raton.

Rabenstein, R. (1999) Transfer function models for multidimensional systems with bounded spatial domains. *Mathematical and Computer Modelling of Dynamical Systems*, **5**(3), 259–278.

Strupczewski, W. and Kundzewicz, Z. (1979) On a method of determination of parameters of conceptual models of open channel flow. *Control and Cybernetics*, **8**(4), 281–295.

Uciński, D. (2012) Sensor network scheduling for identification of spatially distributed processes. *International Journal of Applied Mathematics and Computer Science*, **22**, 25–40.

Wang, B.-Z., Wang, X.-H. and Hong, J.-S. (2005) On the Generalized Transmission-Line Theory. *Journal of Electromagnetic Waves and Applications*, **19**(3), 413–425.

Wu, Ch., Yang, F., Zhou, J. and Ouyang, H. (2012) An Improved Quasi-Analytic Method for Direct Impulse Response Analysis of an Offset Reflector. *Electromagnetics*, **32**(7), 375–388.

Xu, C.-Z. and Sallet, G. (2002) Exponential Stability and Transfer Functions of Processes Governed by Symmetric Hyperbolic Systems. *ESAIM: Control, Optimisation and Calculus of Variations*, **7**, 421–442.

Ziółko, M. (2000) *Modeling of wave phenomena (in Polish).* Poland: AGH University of Science and Technology Press, Kraków.

Zwart, H. (2004) Transfer functions for infinite-dimensional systems. *Systems and Control Letters*, **52**(3-4), 247–255.